Available online at www.sciencedirect.com
SCIENCE DIRECT®
Journal of Catalysis 232 (2005) 395–401
JOURNAL OF CATALYSIS
www.elsevier.com/locate/jcat

Oxygen and carbon monoxide interaction on novel clusters like ruthenium: a WAXS study

W. Vogel [a], N. Alonso-Vante [b,*]

[a] *Fritz-Haber-Institut der Max-Planck-Gesellschaft, Faradayweg 4-6, D-14195 Berlin, and Fachhochschule Brandenburg, Magdeburger Str. 50, 14770 Brandenburg, Germany*

[b] *Laboratory of Electrocatalysis, UMR CNRS 6503, Université de Poitiers, 40 Avenue du Recteur Pineau, F-86022 Poitiers cedex, France*

Received 24 December 2004; revised 3 March 2005; accepted 7 March 2005

Available online 10 May 2005

Abstract

Ruthenium oxide-like (Ru_xO_y) nanoparticles were prepared by the decomposition of carbonyl precursors in organic solvents under mild conditions. CO oxidation over the reduced particles was studied by combined in situ X-ray diffraction and gas-phase analysis. For a sample prepared in dichlorobenzene, in a flow of $CO/O_2 = 0.55$, oxidation of CO started at ca. 70 °C with the simultaneous formation of amorphous surface oxide. On further heating, the CO_2 production increased proportionally with the rate of formation of surface oxide. Below ca. 130 °C the catalyst can be reversibly reduced in CO to the disordered precursor state, average size ca. 2.8 nm. After catalytic performance for 3 h at 180 °C, reduction in CO of partially oxidized Ru_xO_y is accompanied by a burst of CO_2 partial pressure and induces particle growth to $\sim$ 5 nm due to the exothermic heat of the reaction. These results are comparable to earlier results for ruthenium single-crystal surfaces studied under low pressure conditions.

Keywords: Ruthenium; Clusters; Carbon monoxide; Nanoparticles; In situ X-ray diffraction

1. Introduction

Ruthenium nanoparticles (Ru_x) prepared by decomposition of a tris-ruthenium dodecacarbonyl in organic solvents (xylene (Xyl) and 1,2-dichlorobenzene (Dcb)) have proved to be effective electrocatalysts when used as electrode materials for molecular oxygen reduction [1–3]. Their electrocatalytic activity toward oxygen reduction in acid medium has been studied in previous papers [4–6]. Furthermore, in situ electrochemical FTIR spectra of CO adsorbates on such nanoparticles was reported recently [7]. These studies showed that the degree of CO interaction was higher on Ru_x(Xyl) than on Ru_x(Dcb). Recent DRIFT studies on MgO- and SiO_2-supported ruthenium nanoparticles prepared by CVD from $Ru_3(CO)_{12}$ precursor indicated the RuO_2 surface overlayer to be the active component for CO oxidation [8]. In situ X-ray diffraction (XRD) and electrochemical methods were used to characterize our Ru clusters with respect to their oxidation/reduction behavior in an oxygen/hydrogen atmosphere [9]. Reduction of air-exposed samples under mild conditions (H_2, $T \leqslant 150$ °C) leads to what we call a "disordered precursor state" of $\sim$ 2-nm Ru metal particles. The disorder may be related to residual subsurface oxygen, which could also cause stability against the coagulation of this non-ligand-stabilized material. A nanoscaled binary compound Ru_xSe_y prepared similarly from carbonyl precursors was found to exhibit extraordinary oxygen resistance and structural stability [10].

There are a vast number of both experimental [11–15] and theoretical [16,17] surface-related studies on ruthenium single crystals under UHV conditions. Some of these studies have been performed recently in the presence of oxygen and carbon monoxide at the Ru(0001) surface, even under high-pressure conditions [11]. However, the complex behavior of

* Corresponding author. Fax: +33 (0)54945-3580.
E-mail address: nicolas.alonso.vante@univ-poitiers.fr (N. Alonso-Vante).

0021-9517/$ – see front matter
doi:10.1016/j.jcat.2005.03.017

ruthenium in its nanodivided form is still a matter of discussion.

It is generally agreed that the catalytic oxidation of carbon monoxide over platinum-group metals proceeds via the so-called Langmuir–Hinshelwood mechanism. However, in contrast to other platinum-group metals such as Pt, Rh, and Pd, ruthenium is the least active metal for CO oxidation under UHV conditions, but its reaction rate under high-pressure and oxidizing conditions is exceptionally high [12]. Therefore, ruthenium appears to be a nice example of a catalyst that exhibits the so-called pressure gap phenomenon. For Ru(0001) surfaces it has been shown that the reaction probability increases by a factor of 100 beyond an oxygen load of 3 ML [13]. It is suggested that subsurface oxygen destabilizes surface oxygen because of the onset of oxide formation. The conversion of these subsurface oxygen atoms into a regular Ru_xO_y phase takes place at temperatures as high as 900–1150 K [14]. Böttcher and Niehus have studied the conditions needed to promote the formation of subsurface oxygen on Ru(0001) in very large oxygen quantities (partial pressure of 10^{-2} mbar) [11]. Surface roughness was found to have considerable influence on the capacity for oxygen penetration. In a more recent paper, the oxygen-rich Ru(0001) surface was found to consist of patches of (1×1)O overlayers in coexistence with patches of RuO_2 with (110) orientation. It is supposed that only the RuO_2(110) domains are able to oxidize CO molecules at high conversion rates, whereas chemisorbed O overlayers are virtually inactive with respect to CO oxidation [15].

In this work we present gas-phase studies of the above-mentioned material in the presence of an oxygen and/or carbon monoxide mixture. In situ X-ray diffraction, combined with on-line monitoring of reaction products, has turned out to be a unique technique for the study of gas-phase catalytic reactions [18,19]. None of the usual techniques applied in catalysis research allow the direct observation of nanocrystalline catalyst particles with respect to their structural changes under reaction conditions. This has not been done so far. For instance, this technique has led to unraveling of the mechanism of the chemical oscillations that occur during CO oxidation over platinum [19]. In an earlier work we used the technique to study CO oxidation over surfactant-stabilized bimetallic PtRu alloy colloids [18].

2. Experimental

2.1. Sample preparation

The ruthenium nanoparticles were elaborated under mild conditions in organic solutions, from $Ru_3(CO)_{12}$, as described, for example, in Refs. [3,5]. In short, the chemical precursor ($Ru_3(CO)_{12}$ (from Alpha no. 617002) was dissolved either in xylene (Xyl, Merck no. 8687.1000) or in 1,2-dichlorobenzene (Dcb, Merck no. 6.03298.1000). The reaction was performed in a nitrogen atmosphere under refluxing conditions for 20 h. The nanodivided materials in powder form were recovered by filtration on a 0.2-μm PTFE filter, dried with ethyl ether, and kept in vials. The presence of oxygen from air induces the oxidation of ruthenium nanoparticles. Therefore, unless otherwise quoted, such a material exposed to oxygen from air converts to oxide-like ruthenium nanoparticles (Ru_xO_y).

2.2. X-ray diffraction

X-ray patterns were measured with a Guinier powder diffractometer (Huber) in the 45° transmission mode. A Johansson-type Ge monochromator produces a focused monochromatic Cu-$K_{\alpha 1}$ primary beam ($\lambda = 1.5406$ Å).

Structural changes induced by reactive gases at elevated temperatures were studied with a specially designed in situ cell attached to the goniometer [20]. The cell body was made of stainless steel, and the reaction volume of a cylindrical beryllium cover, mounted on a water-cooled flange, corresponded to a reactor volume of 115 cm^3. The powder samples were lightly pressed into pellets (8 mm × 15.5 mm × 0.1 mm in size). These pellets are mechanically unstable and thus were tightly fixed, and permeable for gas, between two 0.1-mm beryllium plates before they were inserted into the sample holder. In the so-called open slit (OS) mode, the counter slit is set to be stationary, for example, at a prominent peak of the target material. In this time-resolved mode in situ studies of particle growth or oxide formation are possible. A quadrupole mass spectrometer (QMS) is connected to the reaction cell by a differential pump transfer line. This allows analysis of the reaction products during X-ray measurements. Note that the QMS signal has a delay of about 100 s with respect to changes in the gas-phase conditions like flow rate or composition. The conditions for the mass flow within the pore system of the compressed catalyst induce concentration gradients and correlated temperature gradients involving nonisothermal conditions of reaction. This makes a quantitative analysis of reaction kinetics impossible, but allows for observations of selected aspects, as will be discussed later.

Some θ-scans were performed ex situ. In this case the samples were fixed between two 3-μm polyethylene foils and measured immediately in ambient conditions. The background-corrected patterns were subjected to the usual angular correction for absorption, polarization, and geometrical factors and plotted versus the reciprocal scattering length, $b = 2\sin(\theta)/\lambda$.

3. Results

3.1. Gas-phase CO oxidation-temperature dependence, Ru_xO_y(Dcb)

The purpose of this study was to correlate the rate of CO oxidation over Ru_xO_y nanoparticles with the rate of oxide

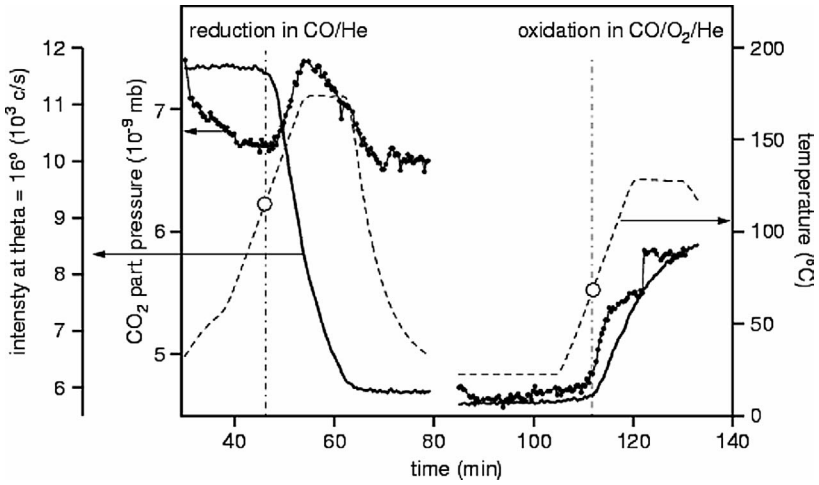

Fig. 1. Intensity around the Ru_xO_y peak and CO_2 partial pressure during reduction in CO versus time and temperature (left side). The reduced sample is then exposed to a flow of O_2/CO/He (right side).

formation/reduction under various conditions of partial pressure and temperature of the reactants.

From previous studies it is known that these catalysts can be reversibly reduced and oxidized under mild conditions to an amorphous Ru_xO_y phase [9]. A sample of Ru_xO_y(Dcb), stored at room temperature in air for several months, was initially pre-reduced in a flow of CO/He (1.22/4.53 ml/min), and the temperature was ramped between room temperature (RT) and 170 °C during reduction. The kinetics of this process can be qualitatively followed by the OS mode (compare Section 2.2); that is, the scattered intensity (I-signal) is measured in a "Bragg window" around the oxide peak ($\theta = 16° \pm 1°$), which serves as a probe for the oxide fraction (this Bragg window is indicated as a vertical bar in the Ru_xO_y diffractogram in Fig. 7). The QMS signal was synchronized with the X-ray unit and measured CO_2 partial pressure in arbitrary units at $m/z = 44$ (CO_2-mass signal). Fig. 1 (left side) displays this experiment. At about 120 °C, marked by a vertical dashed line, the reduction starts. This is evident from the drop in the I-signal. The CO_2 mass signal goes over a maximum during this process. Note that spurious CO_2 in the reactor volume and transfer line produce a $p(CO_2)$ signal that decreases with pumping time. In the actual experiment the pumping time was too short to reduce the CO_2 partial pressure to the final low $p(CO_2)$ background level. This accounts for the high CO_2 signal before the onset of Ru reduction. After cooling the sample to RT we scanned the XRD pattern, which revealed the typical features for the disordered precursor of metallic Ru nanoparticles ~ 2.8 nm in size [9] (Fig. 2, thin line). The diffraction pattern of fully oxidized starting material is shown for comparison (thick line). The diffuse oxide peak disappears and the typical peak for nanoscale Ru metal around $b = 0.44$ Å^{-1} appears instead.

The reduced sample was then exposed to a flow of CO/O_2/He at a flow rate of 4.3/2.4/8.5 ml/min. The result of this treatment is shown on the right side of Fig. 1. On heating, at about 70 °C, ignition of CO oxidation takes place, as indicated by the rising CO_2-mass signal (marked by a vertical line). The I-signal also rises at the ignition point, which indicates the onset of surface oxide formation. Note that this is not a flash-like ignition, in contrast to, for example, that of platinum, where all active sites are blocked by surface CO up to a certain temperature [19]. In this case a high helium flow rate was needed as a "quenching gas" to transport the excess heat away from the catalyst particles and to prevent them from agglomerating and growing. The Ru nanoparticles were slowly re-oxidized under the selected condition of $CO/O_2 < 2$, that is, with a slight excess of oxygen over the stoichiometric ratio.

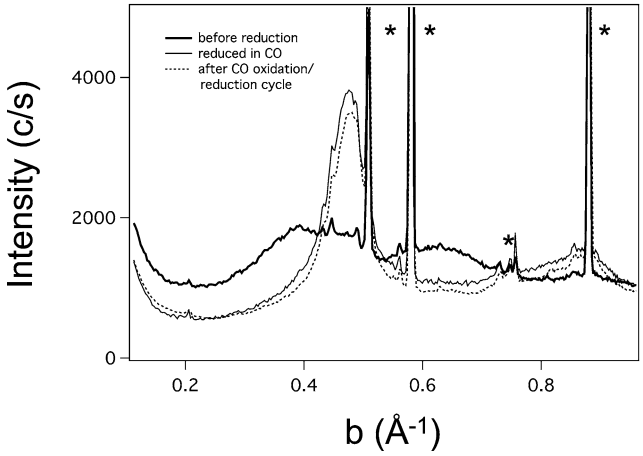

Fig. 2. Diffractogram of the oxidized precursor sample Ru_xO_y(Dcb) after storage for about one month in air at room temperature (thick line), after reduction in CO (thin line), and after the first catalytic performance and consecutive reduction in CO (dashed line). The beryllium plates used to encapsulate the sample produce the narrow peaks (marked by *).

Hereafter, the sample was again reduced in CO. This mild reversible oxidation/reduction treatment converts Ru_xO_y (Dcb) back to the disordered nano-Ru state (Ru_x), since there is no noticeable difference between the two scans

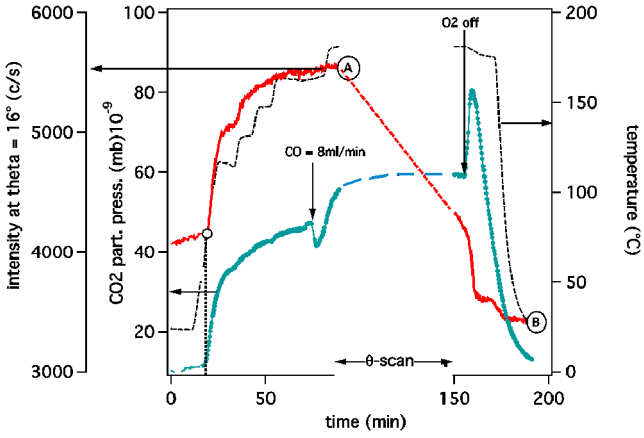

Fig. 3. CO oxidation after three cycles of oxidation/reduction in an O_2/CO/He flow. At point A an intermediate θ-scan was taken under the conditions as specified at this point. When the oxygen flow is switched off (see arrow) the catalyst is rapidly reduced with a short burst of CO_2 pressure (right side).

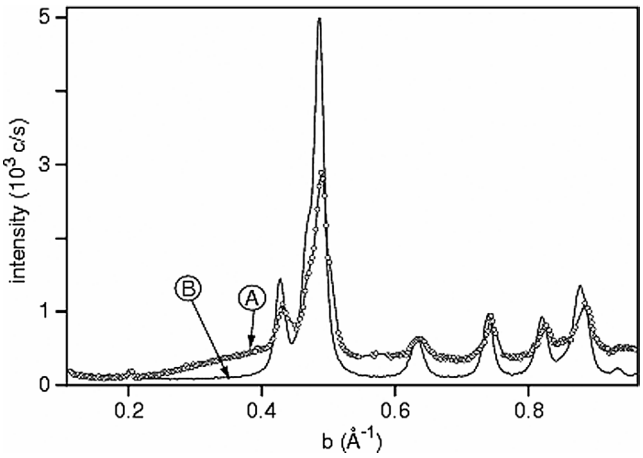

Fig. 4. WAXS patterns of Ru_xO_y(Dcb) taken at point A and point B marked in Fig. 3.

(cf. Fig. 2, dashed line). (Note that in this figure the narrow lines of the beryllium plates used to encapsulate the samples are not cut from the diffraction patterns.)

In a last cycle (after three intermediate ones) CO oxidation continued up to 180 °C, and the flow rates were set to $CO/O_2/He = 4/4/20$ ml/min, that is, to oxidizing conditions (Fig. 3). Again CO oxidation was observed as described in Fig. 1, with ignition at ca. 70 °C and an initially rapid increase in $P_{(CO_2)}$ and surface oxide formation. Both processes approached saturation values as the temperature was increased. At the point marked by an arrow, the CO flow was switched to 8 ml/min, that is, to a more reductive state, which induced an increase in the CO_2 production. A θ-scan was taken under the actual conditions of gas composition/flow and temperature at point A of the figure (duration 50 min). During this period a partial reduction of the catalyst took place. This is obvious from the lowering of the I-signal after the θ-scan was started at point A (dashed lines connect these points in the figure). Shortly after the θ-scan the oxygen flow was shut off as marked in the figure. As a consequence the sample was rapidly reduced: the I-signal dropped, and the burst-like CO_2 signal ran above maximum before dropping to its background level. It appears, therefore, that only oxygen from the gas phase is needed to maintain a certain level of surface oxide, whereas the surface oxide itself is the catalytic active zone of the ruthenium catalyst.

Fig. 4 shows a θ-scan taken ex situ at RT at point B of Fig. 3 and compared with that of point A. Despite the fact that scan A was taken under nonstationary conditions, the diffraction pattern evidently shows the presence of oxide, represented by the high background level. It is important to note that this oxide-related background is "X-ray amorphous" and shows no crystallinity. We believe that the oxide forms as an amorphous overlayer on top of the metallic ruthenium particles. At point B, that is, after the flash-like reduction of this overlayer, the Ru_x particles grow irreversibly and represent a well-developed Ru phase.

3.2. *Partial pressure dependence, Ru_xO_y(Xyl)*

A Ru_xO_y(Xyl) sample, generated from Ru_x(Xyl) previously stored in air for 8 months at RT, was reduced in flowing CO at 200 °C (see Fig. 5), and a θ-scan was taken under these conditions after the sample was cooled to RT. Again the diffraction curve was very similar to that of Ru_x(Xyl) reduced in pure hydrogen at 95 °C, which we have called the disordered precursor state of nano-ruthenium [4,9]. However, for CO used as a reducing agent, a much higher temperature was needed to end at the same state of reduction.

The following experiment was intended to study the effect of the O_2/CO partial pressures on the oxidation of the primarily reduced Ru_x cluster surface. For this purpose the temperature was held constant at 200 °C, and both the I- and CO_2-signals were measured as a function of time and the flow ratio $c = O_2/CO$, which was changed stepwise (Fig. 6). We started with a pure CO flow, which was kept constant at 20 ml/min throughout the whole experiment, while the oxygen flow was increased/decreased between $c = 0$ and 1.

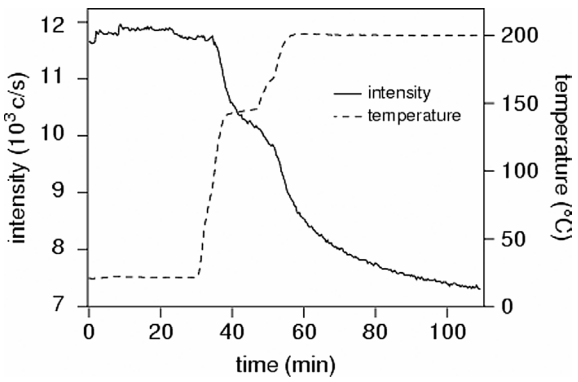

Fig. 5. Intensity around the Ru_xO_y peak (I-signal) during reduction of fully oxidized Ru_xO_y(Xyl) in carbon monoxide versus time and temperature.

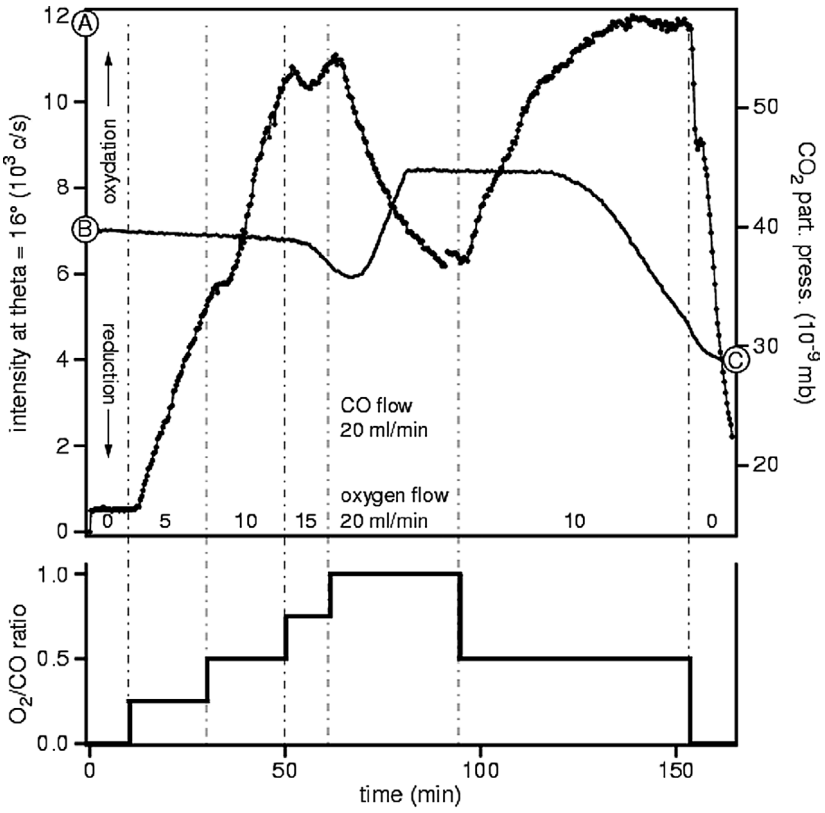

Fig. 6. I-signal (solid line) at the ruthenium oxide 'Bragg window' during CO oxidation at constant 200 °C versus time and flow ratios $c = O_2/CO$ (stair case curve). The CO_2 partial pressure is shown as a separate curve (symbols).

For $c = 0.25$, that is, with CO in excess, CO oxidation is indicated by a linearly increasing CO_2 signal. The response time of the QMS to changes in partial pressures as for $m/z = 44$ is much faster than this increase; that is, the induction time to maximum activity is on the order of hours. Under these conditions we do not observe notable surface oxidation, which would appear as a rising I-signal. Surprisingly, an increase from $c = 0.5$ to 0.75 induces a drop in the I-signal, which, however, reverts to a rising I-signal (oxidation) with a further increase in the O_2/CO ratio to $c = 1$. In this domain, where oxygen is in excess over the stoichiometric ratio $c = 0.5$, the CO_2 production decreases. After a certain reaction time the oxidation of the Ru surface stops abruptly, which is indicated by the horizontal slope of the I-signal. At this point an equilibrium state of oxidation is apparently reached.

When c was switched back to the stoichiometric ratio of 0.5, the CO_2 production rate increased again; that is, the partially oxidized catalyst was still active for CO oxidation. After a certain induction time, however, the I-signal dropped again to a much lower level than that observed at the beginning. This behavior is attributed to a secondary effect related to reduction and a structural rearrangement/growth to more perfect cluster morphology (cf. Fig. 7, curve C). Most likely this growth process is induced by local overheat of the exothermic CO oxidation and is probably also the cause of the first drop of the I-signal in Fig. 6. The exothermic heat of the reaction cannot be dissipated fast enough to prevent the clusters from sintering. In contrast, during the pretreatment of the catalyst for more than 1 h in pure CO at 200 °C, the particles did not grow, but transformed into the reduced

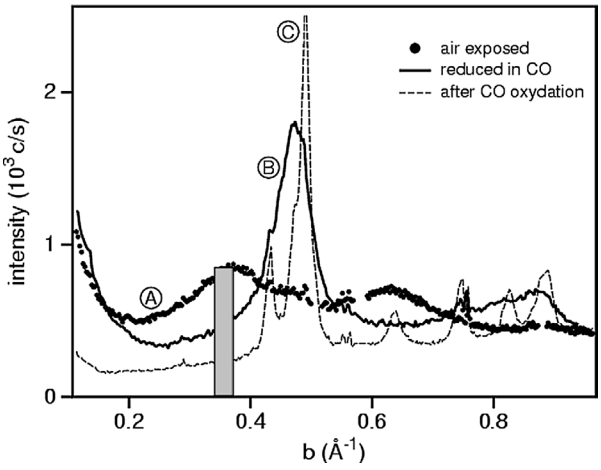

Fig. 7. WAXS patterns of RuO_x(Xyl) after different treatments. (A): stored in air for 8 months (•), (B): reduced in CO at 200 °C (—), and (C): After catalytic CO oxidation at 200 °C for ∼ 50 min (- - -). The vertical bar indicates the 'Bragg window' for the intensity measurements, i.e., the I-signal shown in Figs. 1, 3, 5, and 6.

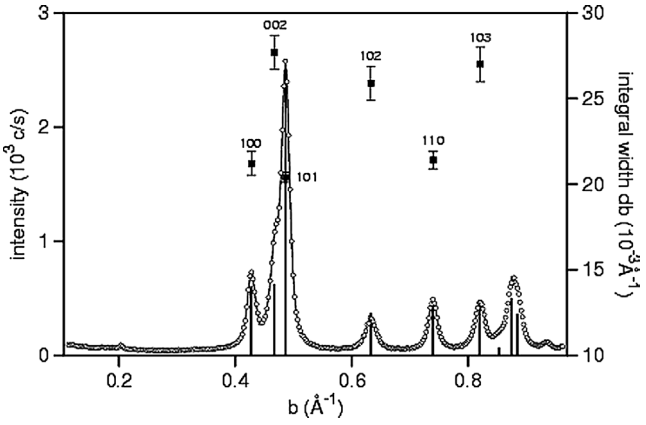

Fig. 8. Line profile analysis of pattern B in Fig. 4 by Pearson VII functions (solid line). The integral line width (d*b*) deduced from the fit is plotted on the same abscissa on the right axis.

precursor state. Fig. 7 compares the diffraction curves taken at the points labeled (A), (B), and (C) in Fig. 6.

3.3. Structural features of Ru_x particles after CO oxidation

We have performed a line profile analysis of scan B in Fig. 4 with the use of Pearson VII functions to fit the first six peaks (solid lines in Fig. 8). The related integral line width (*db*) is plotted versus peak position (right axis of Fig. 8). One can extract the following information from the line width:

(i) Lines *h0l*, $l = 1, 2, 3$ increase in width according to stacking faults of the (001)-planes. The stacking fault probability is calculated to be $\sim 1\%$. This means that about one fault occurs in the stacking at every 100 net planes.

(ii) The *002*-line is much broader than lines *100*, *110*. This relates to a raft-like crystallite shape with a mean lateral size $L_a = 1/\mathrm{d}b(100) = 48$ Å and $L_c = 1/\mathrm{d}b(002) = 36$ Å along the *c*-axis direction. Since the (002) netplane has a spacing $d_{002} = 2.138$ Å, each crystallite consists of an average of 17 planes. This means that only a few of the crystallites contain one stacking defect.

4. Discussion

4.1. Nanoprecursor stability

Previous studies [3–5,9] showed the surprisingly high stability of nanocrystalline ruthenium under mild reducing conditions. In this state we can exclude the presence of residual amorphous ruthenium oxide, but not the presence of subsurface oxygen. The method of preparation and the rather severe pretreatment conditions exclude the presence of organic ligands that may protect the surface. We believe that oxygen is still bound to the surface or is present as a subsurface species and prevents the nanodivided material from coagulating, even under highly reductive conditions (200 °C, 1 bar of CO). Subsurface oxygen would also explain the high degree of disorder found in the precursor state of this material [9]. From single-crystal studies of ruthenium it is well known that chemisorbed oxygen can be fully removed only under extreme conditions, that is, at $T > 1000$ °C under UHV conditions [21].

The XRD experiments presented here are not intended to give a detailed picture of the kinetics involved at the gas/surface interface of the ruthenium nanoparticles. Unfavorable conditions of heat and mass transport and the nonisothermal reaction condition set limitations that may be studied much better in conventional catalyst reactor systems, particularly since the particles are not dispersed on a porous support material that supports gas diffusion. An enhanced surface sensitivity is of course simply related to the small size of the reacting particles. The experiments conducted in this work, however, do shed some light on the complex processes of surface oxidation/reduction and particle growth during reaction that are not available otherwise.

It appears that many of the results that have recently been derived from single-crystal studies do in fact apply likewise to ruthenium in its nanodivided form under high-pressure conditions. Surface oxide plays a decisive role in the ability of ruthenium to catalyze CO oxidation. For Ru_x(Dcb) the rate of CO_2 production increases at $T \geqslant 70$ °C proportionally to the amount of surface oxide formed over a previously reduced catalyst. Very similar results have been observed earlier on 2.3 nm Pt–Ru (1:1) alloy nanoparticles [18]. In a 2:1 CO/O_2 flow, CO oxidation requires a higher temperature than 220 °C, and surface oxidation is observed only above 280 °C.

A direct proof of the role of chemically bonded oxygen in CO oxidation is apparent from Fig. 3. The CO_2 rate becomes constant at $t = 150$ min, $O_2/CO = 0.5$. This means that the buildup of surface oxide by consumption of gas-phase oxygen and the oxide decay by extraction of oxygen to form CO_2 with chemisorbed CO have reached equilibrium. If the oxygen supply of the gas phase is switched off, the latter process is no longer "inhibited" by the former process, as indicated by a rapid increase in CO_2 partial pressure. This reductive reaction lasts until all surface oxide is completely consumed (point B in Fig. 3).

The apparent contradiction of the observed activity of a reduced Ru_x(Xyl) sample at $T = 200$ °C without simultaneous oxide formation can be related to the presence of some residual surface oxide or subsurface oxygen that has not been fully removed by the described reduction procedure. Surface oxide is formed only with oxygen in excess, for example, $O_2/CO \geqslant 0.75$. In this experiment He was not used as a carrier gas, since it could have affected at least heat dissipation, thus preventing the thermal activation of oxide formation.

An amazing aspect is the apparent equilibrium state of surface oxide formation. It is reached after a certain induc-

tion period (time = 81 min) and persists for a certain period, even when the O_2 partial pressure is lowered to $O_2/CO = 0.5$ (Fig. 6). Further work is needed to understand this phenomenon.

4.2. Solid/liquid interface

The surface reaction toward CO oxidation onto Ru_x(Xyl) and Ru_x(Dcb) on the solid/gas interface reflects, to some extent, a similar behavior when such surfaces form an electrochemical interface (solid/liquid). In fact, as reported in an earlier work [9], a striking difference in charge stored in the electrochemical double layer between the "reduced" states, that is, of Ru_x(Xyl) and Ru_x(Dcb), was observed. More charges (ca. 10 times) are accumulated on Ru_x(Xyl) than on Ru_x(Dcb). Such an effect can be due to the fact that the species present in the electrolyte (e.g., H^+, OH^-) interact differently (adsorption process) according to the state of electrode surface, leading to so-called pseudocapacitance. On the other hand, it was observed that the amount of CO adsorbed to Ru_x(Xyl) in an electrochemical cell was also higher than adsorbed to Ru_x(Dcb) [7]. Since the measured CO_{ads} vibration frequency from FTIR measurements, in reflexion mode, was similar on the two samples, we arrive at the conclusion that the CO species adsorb easily to Ru_x(Xyl) by displacing. other molecules responsible for the stored charge (pseudocapacitance) in the double layer. This phenomenon also takes place, although to a lesser extent, on the oxidized material. This complex interplay between the species in the electrolyte and the state of the surface of Ru nanoparticle reflects the catalytic behavior depicted in Figs. 1, 3, 5, and 6.

5. Conclusion

It has been shown that in situ X-ray diffraction combined with gas-phase analysis is capable of providing insight into catalytic processes that depend on a partial surface oxidation of the base material. As a matter of fact, nanodivided ruthenium has achieved growing importance as a fuel cell catalyst and in different fields of catalysis such as low-temperature NH_3 synthesis [22] or alkane hydrogenolysis [23]. The pronounced difference between ruthenium, on the one hand, and other group 9 and 10 elements in alkane hydrogenolysis has been pointed out earlier by Paál et al. [24]. The importance of strongly bound oxygen on ruthenium in its interaction with the oxygen-containing groups of cyclohexanol and cyclohexanone has also been reported [25]. The interaction of Ru oxide with the C–OH and –C=O functional groups may be analogous to that reported here for carbon monoxide.

The present work shows that the catalytic behavior of ruthenium nanoparticles depends on the synthesis conditions and pretreatment. This difference is verified when xylene and dichlorobenzene are used as solvents. It is suggested that subsurface oxygen species play a decisive role in this difference. More experiments of this type are of course needed to get a full understanding of the underlying mechanisms (e.g., for CO oxidation). In these experiments it would be important to avoid conditions that lead to particle agglomeration, since meaningful data can be gained only at a constant dispersion of the active catalyst surface.

Acknowledgments

N.A.V. expresses his thanks to the Alexander von Humboldt Stiftung and the Max Planck Society for funding his stay at the Fritz-Haber-Institut. The authors are grateful to Drs. V. Le Rhun and A.C. Boucher for their technical assistance in the sample preparation.

References

[1] N. Alonso-Vante, M. Giersig, H. Tributsch, J. Electrochem. Soc. 138 (1991) 639.
[2] O. Solorza-Feria, K. Ellmer, M. Giersig, N. Alonso-Vante, Electrochim. Acta 40 (1995) 567.
[3] V. Le Rhun, E. Garnier, S. Pronier, N. Alonso-Vante, Electrochem. Commun. 2 (2000) 475.
[4] V. Le Rhun, E. Garnier, W. Vogel, N. Alonso-Vante, 51st Meeting of ISE, Warsaw, Poland, 3–5 September 2000.
[5] V. Le Rhun, N. Alonso-Vante, J. New. Mater. Electrochem. Syst. 3 (2000) 331.
[6] T.J. Schmidt, U. Paulus, H.A. Gasteiger, N. Alonso-Vante, R.J. Behm, J. Electrochem. Soc. 147 (2000) 2620.
[7] A.-C. Boucher, V. Le Rhun, F. Hahn, N. Alonso-Vante, J. Electroanal. Chem. 554–555 (2003) 379.
[8] J. Aßmann, E. Löffler, A. Birkner, M. Muhler, Catal. Today 85 (2003) 235.
[9] W. Vogel, V. Le Rhun, E. Garnier, N. Alonso-Vante, J. Phys. Chem. B 105 (2001) 5238.
[10] F. Dassenoy, W. Vogel, N. Alonso-Vante, J. Phys. Chem. B 106 (2002) 12152.
[11] A. Böttcher, H. Niehus, J. Chem. Phys. 110 (1999) 3186.
[12] C.H.F. Penden, D.W. Goodman, J. Phys. Chem. 90 (1986) 1360.
[13] A. Böttcher, H. Niehus, S. Schwegmann, H. Over, G. Ertl, J. Phys. Chem. B 101 (1997) 11185.
[14] A. Böttcher, H. Conrad, H. Niehus, J. Chem. Phys. 112 (2000) 4779.
[15] Y.D. Kim, H. Over, G. Krabbes, G. Ertl, Top. Catal. 14 (2001) 95.
[16] K. Reuter, C. Stampfl, M.V. Ganduglia-Pirovan, M. Scheffler, Chem. Phys. Lett. 352 (2002) 311.
[17] M. Todorova, W.X. Li, M.V. Ganduglia-Pirovano, C. Stampfl, K. Reuter, M. Scheffler, Phys. Rev. Lett. 89 (2002) 096103.
[18] W. Vogel, P. Britz, H. Bönnemann, J. Rothe, J. Hormes, J. Phys. Chem. B 101 (1997) 11029.
[19] N. Hartmann, R. Imbihl, W. Vogel, Catal. Lett. 28 (1994) 373.
[20] W. Vogel, Cryst. Res. Technol. 33 (1998) 1141.
[21] A. Böttcher, N. Niehus, Phys. Rev. B 60 (1999) 14396.
[22] F. Rosowski, A. Hornung, O. Hinrichsen, D. Herein, M. Muhler, G. Ertl, Appl. Catal. A 151 (1997) 443.
[23] G.C. Bond, B. Coq, R. Dutatre, J.G. Ruiz, A.D. Hooper, M.G. Proietti, M.C. Sanchez Sierra, J.C. Slaa, J. Catal. 161 (1996) 480.
[24] Z. Paál, P. Tetenyi, Nature 267 (1977) 234.
[25] M. Dobrovolszky, P. Tetenyi, Z. Paál, J. Catal. 74 (1982) 31.